

---

# Small batch deep reinforcement learning

---

Anonymous Author(s)

Affiliation

Address

email

## Abstract

1 In value-based deep reinforcement learning with replay memories, the batch size  
2 parameter specifies how many transitions to sample for each gradient update.  
3 Although critical to the learning process, this value is typically not adjusted when  
4 proposing new algorithms. In this work we present a broad empirical study that  
5 suggests *reducing* the batch size can result in a number of significant performance  
6 gains; this is surprising, as the general tendency when training neural networks  
7 is towards larger batch sizes for improved performance. We complement our  
8 experimental findings with a set of empirical analyses towards better understanding  
9 this phenomenon.

## 10 1 Introduction

11 One of the central concerns for deep reinforcement learning (RL) is how to efficiently make the most  
12 use of the collected data for policy improvement. This is particularly important in online settings,  
13 where RL agents learn while interacting with an environment, as interactions can be expensive. Since  
14 the introduction of DQN [Mnih et al., 2015], one of the core components of most modern deep RL  
15 algorithms is the use of a finite *replay memory* where experienced transitions are stored. During  
16 learning, the agent samples mini-batches from this memory to update its network parameters.

17 Since the policy used to collect transitions is changing throughout learning, the replay memory  
18 contains data coming from a mixture of policies (that differ from the agent’s current policy), and  
19 results in what is known as *off-policy* learning. In contrast with training data for supervised learning  
20 problems, online RL data is highly *non-stationary*. Still, at any point during training the replay  
21 memory exhibits a distribution over transitions, which the agent samples from at each learning step.  
22 The number of sampled transitions at each learning step is known as the *batch size*, and is meant to  
23 produce an unbiased estimator of the underlying data distribution. Thus, in theory, larger batch sizes  
24 should be more accurate representations of the true distribution.

25 Some in the supervised learning community suggest that learning with large batch sizes leads to  
26 better optimization [Shallue et al., 2019], since smaller batches yield noisier gradient estimations.  
27 Contrastingly, others have observed that larger batch sizes tend to converge to “sharper” optimization  
28 landscapes, which can result in worsened generalization [Keskar et al., 2017]; smaller batches, on the  
29 other hand, seem to result in “flatter” landscapes, resulting in better generalization.

30 Learning dynamics in deep RL are drastically different than those observed in supervised learning,  
31 in large part due to the data non-stationarity mentioned above. Given that the choice of batch size  
32 will have a direct influence on the agent’s sample efficiency and ultimate performance, developing a  
33 better understanding of its impact is critical. Surprisingly, to the best of our knowledge there have  
34 been no studies exploring the impact of the choice of batch size in deep RL. Most recent works have  
35 focused on related questions, such as the number of gradient updates per environment step [Nikishin  
36 et al., 2022, D’Oro et al., 2023, Sokar et al., 2023], but have kept the batch size fixed.

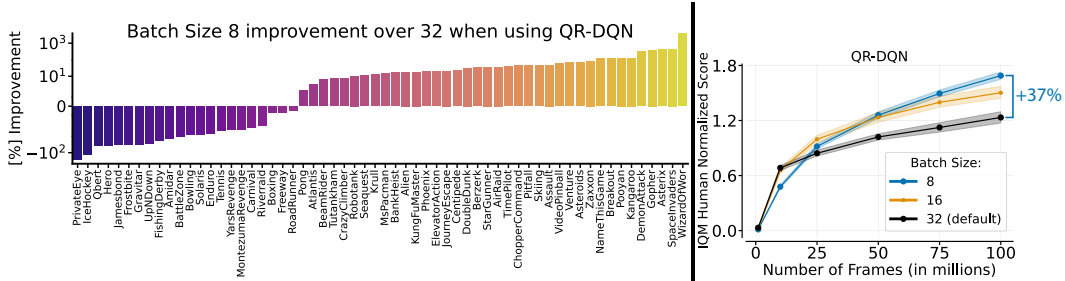


Figure 1: Evaluating QR-DQN [Dabney et al., 2018a] with varying batch sizes over all 60 Atari 2600 games. (Left) Average improvement obtained when using a batch size of 8 over 32 (default); (Right) Aggregate Interquartile Mean [Agarwal et al., 2021] of human normalized scores. All games run for 3 seeds, with shaded areas displaying 95% stratified bootstrap confidence intervals.

37 In this work we conduct a broad empirical study of batch size in online value-based deep reinforcement  
 38 learning. We uncover the surprising finding that *reducing* the batch size seems to provide substantial  
 39 performance benefits and computational savings. We showcase this finding in a variety of agents and  
 40 training regimes (section 3), and conduct in-depth analyses of the possible causes (section 4). The  
 41 impact of our findings and analyses go beyond the choice of the batch size hyper-parameter, and help  
 42 us develop a better understanding of the learning dynamics in online deep RL.

## 43 2 Background

44 A reinforcement learning problem is typically formulated as a Markov decision process (MDP),  
 45 which consists of a 5-tuple  $\langle \mathcal{S}, \mathcal{A}, \mathcal{P}, \mathcal{R}, \gamma \rangle$ , where  $\mathcal{S}$  denotes the state space,  $\mathcal{A}$  denotes the actions,  
 46  $\mathcal{P} : \mathcal{S} \times \mathcal{A} \rightarrow \text{Dist}(\mathcal{S})$  encodes the transition dynamics,  $\mathcal{R} : \mathcal{S} \times \mathcal{A} \rightarrow \mathbb{R}$  is the reward function,  
 47 and  $\gamma \in [0, 1]$  is a discount factor. The aim to learn a *policy*  $\pi_\theta : \mathcal{S} \mapsto \mathcal{A}$  parameterized by  
 48  $\theta$  such that the sum of discounted returns  $\mathbb{E}_{\pi_\theta} [\sum_{t=1}^{\infty} \gamma^t r_t]$  is maximized; here, the state-action  
 49 trajectory  $(s_0, a_0, s_1, a_1, \dots)$  is obtained by sampling an action  $\mathbf{a}_t \sim \pi_\theta(\cdot | s_t)$  and reaching state  
 50  $s_{t+1} \sim \mathcal{P}(\cdot | s_t, \mathbf{a}_t)$  at each decision step  $t$ , and  $r_t \sim \mathcal{R}(\cdot | s_t, \mathbf{a}_t)$ .

51 In value-based methods, the policy is obtained as the argmax of a learned  $Q$ -function:  $\pi_\theta(s) \equiv$   
 52  $\arg \max_{a \in \mathcal{A}} Q_\theta(s, a)$ . This function aims to approximate the optimal state-action values  $Q^*$ , defined  
 53 via the well-known Bellman recurrence:  $Q^*(s_t, \mathbf{a}_t) = \max_{\mathbf{a}'} \mathbb{E}[\mathcal{R}(s_t, \mathbf{a}_t) + \gamma Q^*(s_{t+1}, \mathbf{a}_{t+1})]$ , and  
 54 is typically learned using  $Q$ -learning [Watkins and Dayan, 1992, Sutton and Barto, 2018].

55 To deal with large state spaces, such as all possible images in an Atari 2600 game, Mnih et al.  
 56 [2015] introduced DQN, which combined  $Q$ -learning with deep neural networks to represent  $Q_\theta$ .  
 57 A large *replay buffer*  $D$  is maintained to store experienced transitions, from which mini-batches  
 58 are sampled to perform learning updates [Lin, 1992]. Specifically, *temporal difference learning*  
 59 is used to update the network parameters with the following loss function:  $L(\theta) =_{(s_t, a_t, r, s_{t+1}) \sim D}$   
 60  $[(r + \gamma \max_{a' \in \mathcal{A}} Q_{\bar{\theta}}(s_{t+1}, a_{t+1}) - Q_\theta(s_t, a_t))^2]$ . Here  $Q_{\bar{\theta}}$  is a *target network* that is a delayed  
 61 copy of  $Q_\theta$ , with the parameters synced with  $Q_\theta$  less frequently than  $Q_\theta$  is updated.

62 Since the introduction of DQN, there have been a number of algorithmic advances in deep RL  
 63 agents, in particular those which make use of distributional RL [Bellemare et al., 2017], introduced  
 64 with the C51 algorithm. The Rainbow agent combined C51 with other advances such as multi-step  
 65 learning and prioritized replay sampling [Hessel et al., 2018]. Different ways of parameterizing return  
 66 distributions were proposed in the form of the IQN [Dabney et al., 2018b] and QR-DQN [Dabney  
 67 et al., 2018a] algorithms. For reasons which will be clarified below, most of our evaluations and  
 68 analyses were conducted with the QR-DQN agent.

## 69 3 The small batch effect on agent performance

70 In this section we showcase the performance gains that arise when training with smaller batch sizes.  
 71 We do so first with four standard value-based agents (§3.1), with varying architectures (§3.2), agents

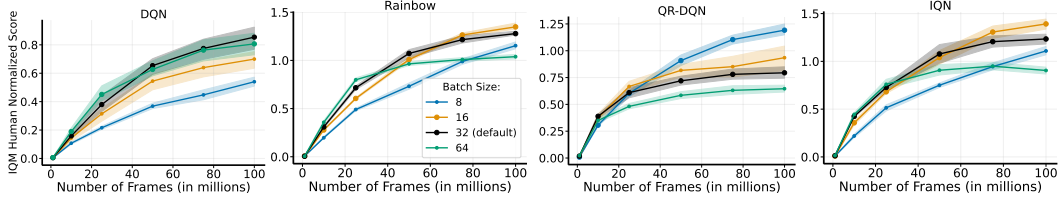


Figure 3: IQM for human normalized scores for DQN, Rainbow, QR-DQN, and IQN. All games run with 3 independent seeds, shaded areas representing 95% confidence intervals.

72 optimized for sample efficiency (§3.3), and with extended training (§3.4). Additionally, we explore  
 73 the impact of reduced batch sizes on exploration (§3.5) and computational cost (§3.6).

74 **Experimental setup:** We use the Jax implementations of RL agents, with their default hyper-  
 75 parameter values, provided by the Dopamine library [Castro et al., 2018]<sup>1</sup> and applied to the Arcade  
 76 Learning Environment (ALE) [Bellemare et al., 2013].<sup>2</sup> It is worth noting that the default batch size is  
 77 32, which we indicate with a **black** color in all the plots below, for clarity. We evaluate our agents on  
 78 20 games chosen by Fedus et al. [2020] for their analysis of replay ratios, picked to offer a diversity  
 79 of difficulty and dynamics. To reduce the computational burden, we ran most of our experiments for  
 80 100 million frames (as opposed to the standard 200 million). For evaluation, we follow the guidelines  
 81 of Agarwal et al. [2021]. Specifically, we run 3 independent seeds for each experiment and report  
 82 the human-normalized *interquantile mean (IQM)*, aggregated over the 20 games, configurations, and  
 83 seeds, with the 95% stratified bootstrap confidence intervals. Note that this means that for most of the  
 84 aggregate results presented here, we are reporting mean and confidence intervals over 60 independent  
 85 seeds. All experiments were run on NVIDIA Tesla P100 GPUs.

### 86 3.1 Standard agents

87 We begin by investigating the impact reducing the  
 88 batch size can have on four popular value-based  
 89 agents, which were initially benchmarked on the  
 90 ALE suite: DQN [Mnih et al., 2015], Rainbow  
 91 [Hessel et al., 2018] (Note that Dopamine uses a  
 92 “compact” version of the original Rainbow agent,  
 93 including only multi-step updates, prioritized re-  
 94 play, and C51), QR-DQN [Dabney et al., 2018a],  
 95 and IQN [Dabney et al., 2018b]. In Figure 3 we can  
 96 observe that, in general, reduced batch size results  
 97 in improved performance. The notable exception  
 98 is DQN, for which we provide an analysis and ex-  
 99 planation for why this is the case below. To verify  
 100 that our results are not a consequence of the set of  
 101 20 games used in our analyses, we ran QR-DQN  
 102 (where the effect is most observed) over the full  
 103 60 games in the suite and report the results in Fig-  
 104 ure 15. Remarkably, a batch size of 8 results in  
 105 significant gains on 38 out of the full 60 games, for an average performance improvement of 98.25%.

### 106 3.2 Varying architectures

107 Although the CNN architecture originally introduced by DQN [Mnih et al., 2015] has been the  
 108 backbone for most deep RL networks, there have been some recent works exploring the effects  
 109 of varying architectures [Espohlt et al., 2018, Agarwal et al., 2022, Sokar et al., 2023]. We  
 110 investigate the small batch effect by varying the QR-DQN architecture in two ways: **(I)** expanding  
 111 the convolutional widths by 4 times (resulting in a substantial increase in the number of parameters),

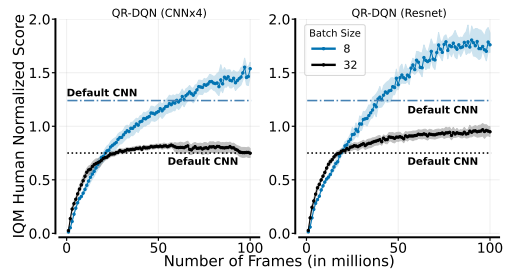


Figure 2: IQM for human normalized scores with varying neural network architectures over 20 games, with 3 seeds per experiment. Shaded areas represent 95% stratified bootstrap confidence intervals.

<sup>1</sup>Dopamine code available at <https://github.com/google/dopamine>.

<sup>2</sup>Dopamine uses sticky actions by default [Machado et al., 2018].

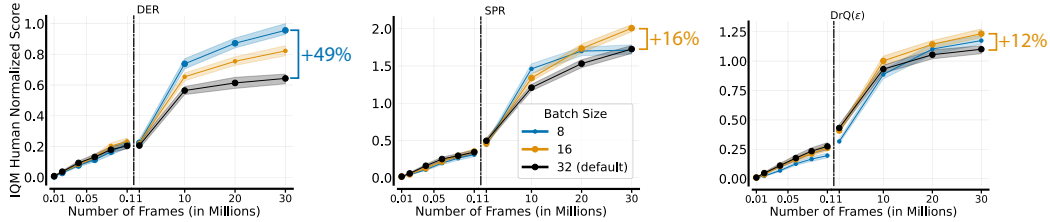


Figure 4: Measured IQM of human-normalized scores on the 26 100k benchmark games, with varying batch sizes, of DER, SPR, and DrQ( $\epsilon$ ). We evaluate performance at 100k agent steps (or 400k environment frames), and at 30 million environment frames, run with 6 independent seeds for each experiment, and shaded areas display 95% confidence intervals.

112 and (2) using the Resnet architecture proposed by Espeholt et al. [2018] (which results in a similar  
 113 number of parameters to the original CNN architecture, but is a deeper network). In Figure 2 we can  
 114 observe that not only do reduced batch sizes yield improved performance, but they are better able to  
 115 leverage the increased number of parameters (CNNx4) and the increased depth (Resnet).

### 116 3.3 Atari 100k agents

117 There has been an increased interest in evaluating Atari agents on very few environment interactions,  
 118 for which Kaiser et al. [2020] proposed the 100k benchmark<sup>3</sup>. We evaluate the effect of reduced  
 119 batch size on three of the most widely used agents for this regime: Data-efficient Rainbow (DER), a  
 120 version of the Rainbow algorithm with hyper-parameters tuned for faster early learning [van Hasselt  
 121 et al., 2019]; DrQ( $\epsilon$ ), which is a variant of DQN that uses data augmentation [Agarwal et al., 2021];  
 122 and SPR, which incorporates self-supervised learning to improve sample efficiency [Schwarzer et al.,  
 123 2020]. For this evaluation we evaluate on the standard 26 games for this benchmark [Kaiser et al.,  
 124 2020], aggregated over 6 independent trials.

125 In Figure 4 we include results both at the 100k benchmark (left side of plots), and when trained  
 126 for 30 million frames. Our intent is to evaluate the batch size effect on agents that were optimized  
 127 for a different training regime. We can see that although there is little difference in 100k, there is a  
 128 much more pronounced effect when trained for longer. This finding suggests that reduced batch sizes  
 129 enables continued performance improvements when trained for longer.

### 130 3.4 Training Stability

131 To further investigate whether reduced batch sizes  
 132 enables continual improvements with longer training,  
 133 we extend the training of QR-DQN up to the  
 134 standard 200 million frames. In Figure 5 we can  
 135 see that training performance tends to plateau for  
 136 the higher batch sizes. In contrast, the smaller  
 137 batch sizes seem to be able to continuously improve their  
 138 performance.

### 139 3.5 Impact on exploration

140 The simplest and most widely used approach for  
 141 exploration is to select actions randomly with a  
 142 probability  $\epsilon$ , as opposed to selecting them greedily  
 143 from the current  $Q_\theta$  estimate. The increased vari-  
 144 ance resulting from reduced batch sizes (as we will  
 145 explore in more depth below) may also result in a  
 146 natural form of exploration. To investigate this, we

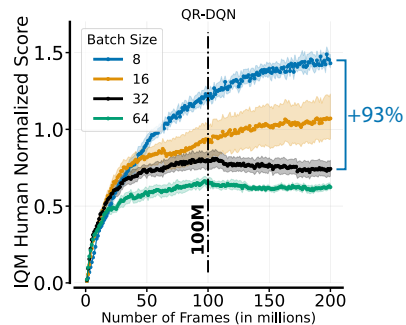


Figure 5: Measuring IQM for human-normalized scores when training for 200 million frames. Results aggregated over 20 games, where each experiment was run with 3 independent seeds and we report 95% confidence intervals.

<sup>3</sup>Here, 100k refers to agent steps, or 400k environment frames, due to skipping frames in the standard training setup.

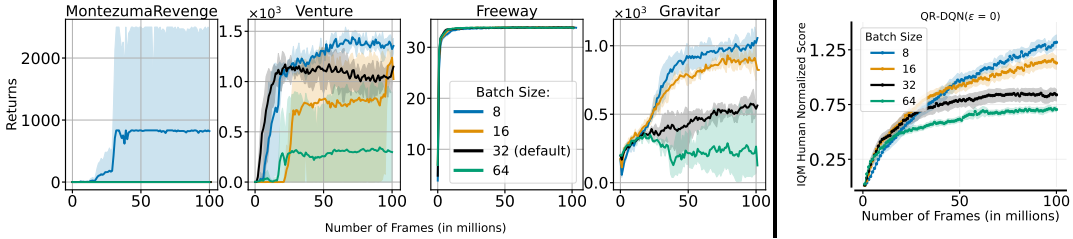


Figure 6: **Left:** Performance of QR-DQN on four hard exploration games with a target  $\epsilon$  value of 0.0, and with varying batch sizes. **Right:** Aggregate IQM of human-normalized scores over 20 games with a target  $\epsilon$  value of 0.0. In all the plots 3 independent seeds were used for each game/batch-size configuration, with shaded areas representing 95% confidence intervals.

147 set the target  $\epsilon$  value to 0.0 for QR-DQN<sup>4</sup>. In Figure 6 we compare performance across four known  
 148 hard exploration games [Bellemare et al., 2016, Taiga et al., 2020] and observe that reduced batch  
 149 sizes tends to result in improved performance for these games.

### 150 3.6 Computational impact

151 Empirical advances in deep reinforcement learning are generally measured with respect to sample  
 152 efficiency; that is, the number of environment interactions required before achieving a certain level of  
 153 performance. It fails to capture computational differences between algorithms. If two algorithms  
 154 have the same performance with respect to environment interactions, but one takes twice as long to  
 155 perform each training step, one would clearly opt for the faster of the two. This important distinction,  
 156 however, is largely overlooked in the standard evaluation methodologies used by the DRL community.

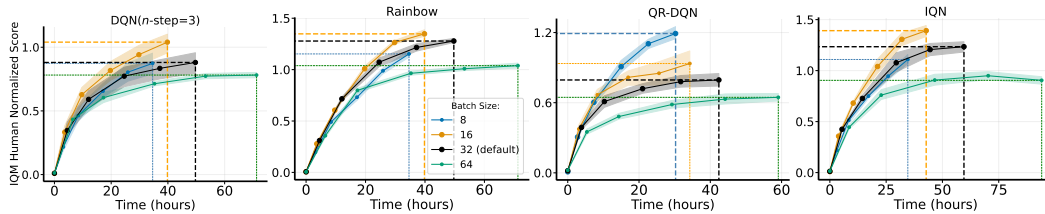


Figure 7: Measuring wall-time versus IQM of human-normalized scores when varying batch sizes in DQN (with  $n$ -step set to 3), Rainbow, QR-DQN, and IQN. Each experiment had 3 independent runs, and the confidence intervals show 95% confidence intervals.

157 We have already demonstrated the performance benefits obtained when reducing batch size, but an  
 158 additional important consequence is the reduction in computation wall-time. Figure 7 demonstrates  
 159 that not only can we obtain better performance with a reduced batch size, but we can do so at a  
 160 fraction of the runtime. As a concrete example, when changing the batch size of QR-DQN from  
 161 the default value of 32 to 8, we achieve both a 50% performance increase and a 29% speedup in  
 162 wall-time.

163 It may seem surprising that smaller batch sizes have a faster runtime, since larger batches presumably  
 164 make better use of GPU parallelism. However, as pointed out by Masters and Luschi [2018], the  
 165 speedups may be a result of a smaller memory footprint, enabling better machine throughput.

<sup>4</sup>Note that we follow the training schedule of Mnih et al. [2015] where the  $\epsilon$  value begins at 1.0 and is linearly decayed to its target value over the first million environment frames.



### Key observations on reduced batch sizes:

- They generally improve performance, as evaluated across a variety of agents and network architectures.
- When trained for longer, the performance gains continue, rather than plateauing.
- They seem to have a beneficial effect on exploration.
- They result in faster training, as measured by wall-time.

166

## 167 4 Understanding the small batch effect

168 Having demonstrated the performance benefits arising from a reduced batch size across a wide  
169 range of tasks, in this section we seek to gain some insight into possible causes. We will focus on  
170 QR-DQN, as this is the agent where the small batch effect is most pronounced (Figure 3). We begin  
171 by investigating possible confounding factors for the small batch effect, and then provide analyses on  
172 the effect of reduced batch sizes on network dynamics.

### 173 4.1 Relation to other hyperparameters

174 **Learning rates** It is natural to wonder whether an improved learning rate could produce the same  
175 effect as simply reducing the batch size. In Figure 8 we explored a variety of different learning rates and  
176 observe that, although performance is relatively stable with a batch size of 32, it is unable to reach  
177 the performance gains obtained with a batch size  
178 of 8 or 16.  
179  
180  
181

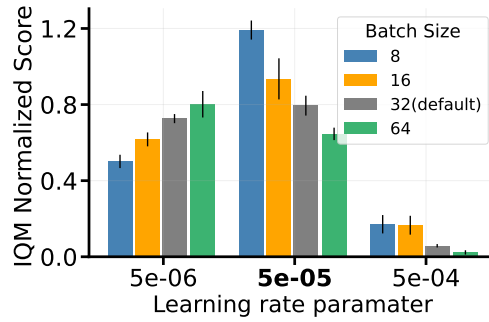


Figure 8: Varying batch sizes for different learning values.

182 **Second order optimizer effects** All our experi-  
183 ments, like most modern RL agents, use the Adam  
184 optimizer [Kingma and Ba, 2015], a variant of  
185 stochastic gradient descent (SGD) that adapts its  
186 learning rate based on the first- and second-order  
187 moments of the gradients, as estimated from mini-batches used for training. It is thus possible that  
188 smaller batch sizes have a second-order effect on the learning-rate adaptation that benefits agent  
189 performance. To investigate this we evaluated, for each training step, performing multiple gradient  
190 updates on subsets of the original sampled batch; we define the parameter *BatchDivisor* as the  
191 number of gradient updates and dividing factor (where a value of 1 is the default setting). Thus,  
192 for a *BatchDivisor* of 4, we would perform 4 gradient updates with subsets of size 8 instead of a  
193 single gradient update with a mini-batch of size 32. With an optimizer like SGD this has no effect (as  
194 they are mathematically equivalent), but we may see differing performance due to Adam’s adaptive  
195 learning rates. Figure 9 demonstrates that, while there are differences, these are not consistent nor  
196 significant enough to explain the performance boost observed.

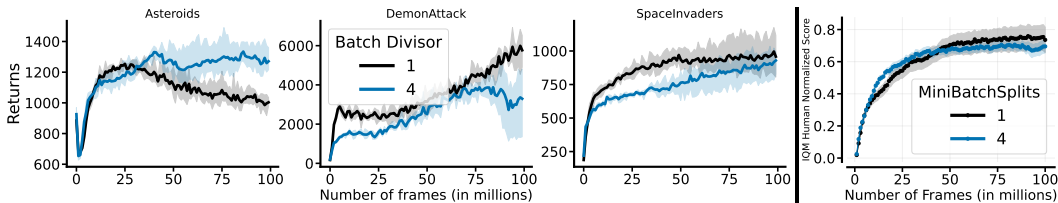


Figure 9: Varying the number of gradient updates per training step, for a fixed batch size of 32.

197 **Relationship with multi-step learning** In Figure 3 we observed that DQN was the only agent  
198 where reducing batch size did not improve performance. Recalling that the Dopamine version of  
199 Rainbow used is simply adding three components to the base DQN agent, we follow the analyses

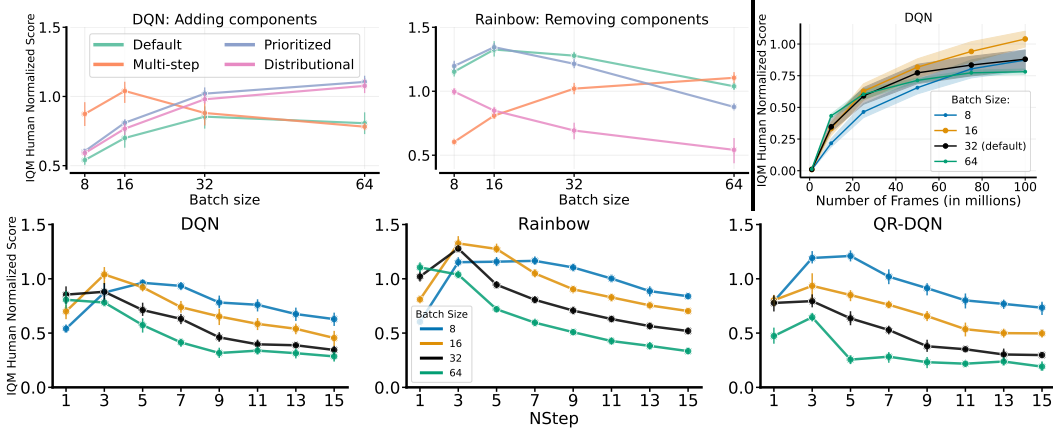


Figure 10: Measured IQM human normalized scores over 20 games with 3 independent seeds for each configuration, displaying 95% stratified bootstrap confidence intervals. **Top left:** Adding components to DQN; **Top center:** Removing components from Rainbow. **Top right:** Aggregate DQN performance with  $n$ -step of 3. **Bottom:** Varying batch sizes and  $n$ -steps in DQN (left), Rainbow (center), and QR-DQN (right).

200 of Hessel et al. [2018] and Ceron and Castro [2021]. Specifically, in Figure 10 (top row) we  
 201 simultaneously add these components to DQN (top left plot) and remove these components from  
 202 Rainbow (top center plot). Remarkably, batch size is inversely correlated with performance *only when*  
 203 *multi-step returns are used*. Given that DQN is the only agent considered here without multi-step  
 204 learning, this finding explains the anomalous findings in Figure 3. Indeed, as the right panel of  
 205 Figure 10 (top row) shows, adding multi-step learning to DQN results in improved performance with  
 206 smaller batch sizes. To further investigate the relationship between batch size and multi-step returns,  
 207 in Figure 10 (bottom row) we evaluate varying both batch sizes and  $n$ -step values for DQN, Rainbow,  
 208 and QR-DQN. We can observe that smaller batch sizes suffer less from degrading performance as the  
 209  $n$ -step value is increased.

**Key insights:**

- The small batch effect does not seem to be a consequence of a sub-optimal choice of learning rate for the default value of 32.
- The small batch effect does not arise due to beneficial interactions with the Adam optimizer.
- The small batch effect appears to be more pronounced with multi-step learning.
- When increasing the update horizon in multi-step learning, smaller batches produce better results.

210

211 **4.2 Analysis of network optimization dynamics**

212 In this section we will focus on three representative games (Asteroids, DemonAttack, and SpaceInvaders), and include results for more games in the supplemental material. In Figure 11 we present the training returns as well as a variety of metrics we collected for our analyses. We will discuss each in more detail below. The first column in this figure displays the training returns for each game, where we can observe the inverse correlation between batch size and performance.

217 **Variance of updates** Intuition suggests that as we decrease the batch size, we will observe an increase in the variance of our updates as our gradient estimates will be noisier. This is confirmed in the second column of Figure 11, where we see an increased variance with reduced batch size.

220 A natural question is whether directly increasing variance results in improved performance, thereby (partially) explaining the results with reduced batch size. To investigate, we added Gaussian noise (at

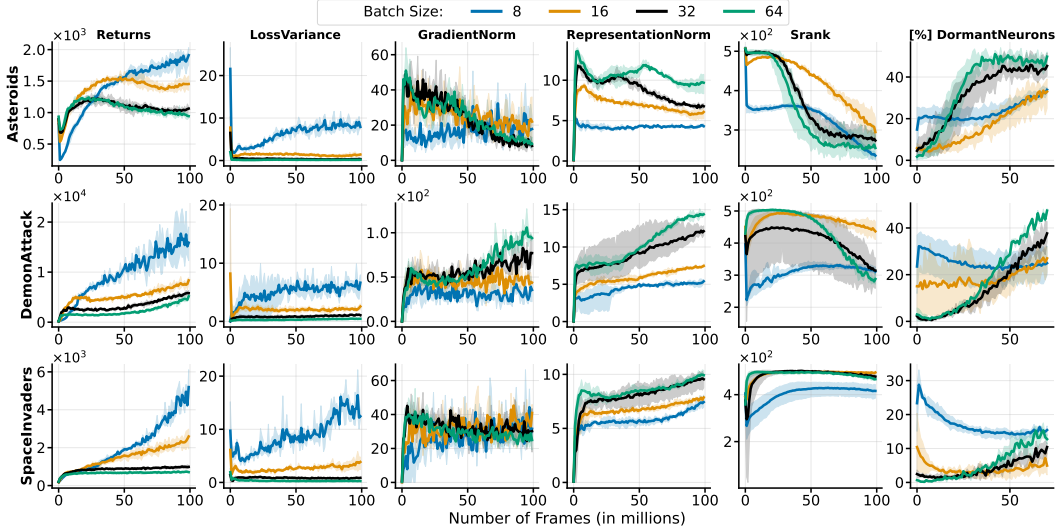


Figure 11: Empirical analyses for three representative games with varying batch sizes. From left to right: training returns, aggregate loss variance, average gradient norm, average representation norm, *srank* [Kumar et al., 2021a], and dormant neurons [Sokar et al., 2023]. All results averaged over 3 seeds, shaded areas represent 95% confidence intervals.

222 varying scales) to the learning target  $Q_{\bar{\theta}}$  (see section 2 for definition). As Figure 12 demonstrates, simply adding noise to the target does provide benefits, albeit with some variation across games.

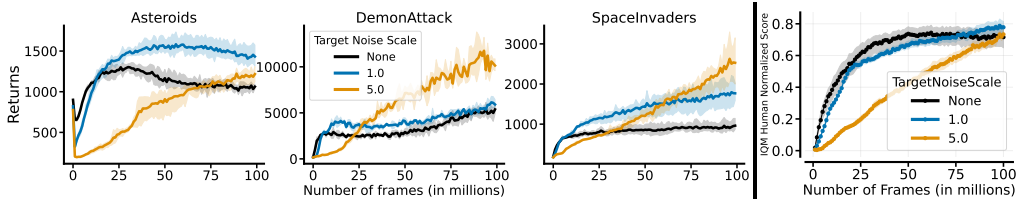


Figure 12: Adding noise of varying scales to the learning target with the default batch size of 32.

223

224 **Gradient and representation norms** Keskar et al. [2017] and Zhao et al. [2022] both argue that  
 225 smaller gradient norms can lead to improved generalization and performance, in part due to less  
 226 “sharp” optimization landscapes. In Figure 11 (third column) we can see that batch size is, in fact,  
 227 correlated with gradient norms, which may be an important factor in the improved performance.

228 There have been a number of recent works suggesting RL representations, taken to be the output  
 229 of the convolutional layers in our networks<sup>5</sup>, yield better agent performance when their norms  
 230 are smaller. Gogianu et al. [2021] demonstrated that normalizing representations yields improved  
 231 agent performance as a result of a change to optimization dynamics; Kumar et al. [2021b] further  
 232 observed that smaller representation norms can help mitigate feature co-adaptation, which can degrade  
 233 agent performance in the offline setting. As Figure 11 (fourth column) shows, the norms of the  
 234 representations are correlated with batch size, which aligns well with the works just mentioned.

235 **Effect on network expressivity and plasticity** Kumar et al. [2021a] introduced the notion of the  
 236 *effective rank* of the representation  $srank_{\delta}(\phi)$ <sup>6</sup>, and argued that it is correlated with a network’s  
 237 expressivity: a reduction in effective rank results in an implicit under-parameterization. The authors  
 238 provide evidence that bootstrapping is the likeliest cause for effective rank collapse (and reduced

<sup>5</sup>This is a common interpretation used recently, for example, by Castro et al. [2021], Gogianu et al. [2021], and Farebrother et al. [2023]

<sup>6</sup> $\delta$  is a threshold parameter. We used the same value of 0.01 as used by Kumar et al. [2021a].



239 performance). Interestingly, in Figure 11 (fifth column) we see that with smaller batch sizes *srank*  
240 collapse occurs earlier in training than with larger batch sizes. Given that there is mounting evidence  
241 that deep RL networks tend to overfit during training [Dabney et al., 2021, Nikishin et al., 2022,  
242 Sokar et al., 2023], it is possible that the network is better able to adapt to an earlier rank collapse  
243 than to a later one.

244 To further investigate the effects on network expressivity, we measured the fraction of *dormant*  
245 *neurons* (neurons with near-zero activations). Sokar et al. [2023] demonstrated that deep RL agents  
246 suffer from an increase in the number of dormant neurons in their network; further, the higher the  
247 level of dormant neurons, the worse the performance. In Figure 11 (rightmost column) we can see  
248 that, although the relationship with batch size is not as clear as with some of the other metrics, smaller  
249 batch sizes appear to have a much milder increase in their frequency. Further, there does appear to be  
250 a close relationship with the measured *srank* findings above.

#### Key insights:

- Reduced batch sizes result in increased variance of losses and gradients. This increased variance can have a beneficial effect during training.
- Smaller batch sizes result in smaller gradient and representation norms, which tend to result in improved performance.
- Smaller batch sizes seem to result in networks that are both more expressive and with greater plasticity.

251

## 252 5 Conclusions

253 In online deep RL, the amount of data sampled during each training step is crucial to an agent’s  
254 learning effectiveness. Common intuition would lead one to believe that larger batches yield better  
255 estimates of the data distribution and yield computational savings due to data parallelism on GPUs.  
256 Our findings here suggest the opposite: the batch size parameter generally alters the agent’s learning  
257 curves in surprising ways, and reducing the batch size below its standard value is often beneficial.

258 From a practical perspective, our experimental results make it clear that the effect of batch size  
259 on performance is substantially more complex than in supervised learning. Beyond the obvious  
260 performance and wall-time gains we observe, changing the batch size appears to have knock-on effects  
261 on exploration as well as asymptotic behaviour. Figure 8 hints at a complex relationship between  
262 learning rate and batch size, suggesting the potential usefulness of “scaling laws” for adjusting these  
263 parameters appropriately.

264 Conversely, our results also highlight a number of theoretically-unexplained effects in deep rein-  
265 forcement learning. For example, one would naturally expect that increasing the batch size should  
266 increase variance, and eventually affect prediction accuracy. That its effect on performance, both  
267 transient and asymptotic, should so critically depend on the degree to which bootstrapping occurs  
268 (as in  $n$ -step returns; Figure 10) suggest that gradient-based temporal-difference learning algorithms  
269 need a fundamentally different analysis from supervised learning methods.

### 270 5.1 Future Work

271 Our focus in this paper has been on value-based online methods. This raises the question of whether  
272 our findings carry over to actor-critic methods, and different training scenarios such as offline RL  
273 [Levine et al., 2020] and distributed training [Stooke and Abbeel, 2018]. While similar findings are  
274 likely for actor-critic methods, the dynamics are sufficiently different in offline RL and in distributed  
275 training that it would likely require a different investigative and analytical approach.

276 Our work has broader implications than just the choice of the batch size hyper-parameter. For  
277 instance, our findings on the impact of variance on performance suggest a promising avenue for  
278 new algorithmic innovations via the explicit injection of variance. Most exploration algorithms  
279 are designed for tabular settings and then adapted for deep networks; our results in section 3.5  
280 suggest there may be opportunities for exploratory algorithms designed specifically for use with  
281 neural networks. We hope our analyses can prove useful for further advances in the development and  
282 understanding of deep networks for reinforcement learning.

## 283 References

- 284 Rishabh Agarwal, Max Schwarzer, Pablo Samuel Castro, Aaron Courville, and Marc G Bellemare.  
285 Deep reinforcement learning at the edge of the statistical precipice. In *Thirty-Fifth Conference on*  
286 *Neural Information Processing Systems*, 2021.
- 287 Rishabh Agarwal, Max Schwarzer, Pablo Samuel Castro, Aaron Courville, and Marc G Bellemare.  
288 Beyond tabula rasa: Reincarnating reinforcement learning. In *Thirty-Sixth Conference on Neural*  
289 *Information Processing Systems*, 2022.
- 290 M. G. Bellemare, Y. Naddaf, J. Veness, and M. Bowling. The arcade learning environment: An  
291 evaluation platform for general agents. *Journal of Artificial Intelligence Research*, 47:253–279,  
292 jun 2013. doi: 10.1613/jair.3912.
- 293 Marc Bellemare, Sriram Srinivasan, Georg Ostrovski, Tom Schaul, David Saxton, and Remi Munos.  
294 Unifying count-based exploration and intrinsic motivation. In D. Lee, M. Sugiyama, U. Luxburg,  
295 I. Guyon, and R. Garnett, editors, *Advances in Neural Information Processing Systems*, vol-  
296 ume 29. Curran Associates, Inc., 2016. URL [https://proceedings.neurips.cc/paper\\_](https://proceedings.neurips.cc/paper_files/paper/2016/file/afda332245e2af431fb7b672a68b659d-Paper.pdf)  
297 [files/paper/2016/file/afda332245e2af431fb7b672a68b659d-Paper.pdf](https://proceedings.neurips.cc/paper_files/paper/2016/file/afda332245e2af431fb7b672a68b659d-Paper.pdf).
- 298 Marc G. Bellemare, Will Dabney, and Rémi Munos. A distributional perspective on reinforcement  
299 learning. In *Proceedings of the 34th International Conference on Machine Learning - Volume 70*,  
300 ICML’17, page 449–458, 2017.
- 301 Pablo Samuel Castro, Subhodeep Moitra, Carles Gelada, Saurabh Kumar, and Marc G. Bellemare.  
302 Dopamine: A Research Framework for Deep Reinforcement Learning. 2018. URL [http:](http://arxiv.org/abs/1812.06110)  
303 [//arxiv.org/abs/1812.06110](http://arxiv.org/abs/1812.06110).
- 304 Pablo Samuel Castro, Tyler Kastner, Prakash Panangaden, and Mark Rowland. MICO: Learning  
305 improved representations via sampling-based state similarity for Markov decision processes. In  
306 *Advances in Neural Information Processing Systems*, 2021.
- 307 Johan Samir Obando Ceron and Pablo Samuel Castro. Revisiting rainbow: Promoting more in-  
308 sightful and inclusive deep reinforcement learning research. In Marina Meila and Tong Zhang,  
309 editors, *Proceedings of the 38th International Conference on Machine Learning*, volume 139 of  
310 *Proceedings of Machine Learning Research*, pages 1373–1383. PMLR, 18–24 Jul 2021. URL  
311 <https://proceedings.mlr.press/v139/ceron21a.html>.
- 312 W. Dabney, M. Rowland, Marc G. Bellemare, and R. Munos. Distributional reinforcement learning  
313 with quantile regression. In *AAAI*, 2018a.
- 314 Will Dabney, Georg Ostrovski, David Silver, and Remi Munos. Implicit quantile networks for  
315 distributional reinforcement learning. In *Proceedings of the 35th International Conference on*  
316 *Machine Learning*, volume 80 of *Proceedings of Machine Learning Research*, pages 1096–1105.  
317 PMLR, 2018b.
- 318 Will Dabney, Andre Barreto, Mark Rowland, Robert Dadashi, John Quan, Marc G. Bellemare, and  
319 David Silver. The value-improvement path: Towards better representations for reinforcement  
320 learning. In *Proceedings of the AAAI Conference on Artificial Intelligence*, 2021.
- 321 Pierluca D’Oro, Max Schwarzer, Evgenii Nikishin, Pierre-Luc Bacon, Marc G Bellemare, and  
322 Aaron Courville. Sample-efficient reinforcement learning by breaking the replay ratio barrier.  
323 In *The Eleventh International Conference on Learning Representations*, 2023. URL [https:](https://openreview.net/forum?id=OpC-9aBBVJe)  
324 [//openreview.net/forum?id=OpC-9aBBVJe](https://openreview.net/forum?id=OpC-9aBBVJe).
- 325 Lasse Espeholt, Hubert Soyer, Rémi Munos, Karen Simonyan, Volodymyr Mnih, Tom Ward, Yotam  
326 Doron, Vlad Firoiu, Tim Harley, Iain Dunning, Shane Legg, and Koray Kavukcuoglu. IMPALA:  
327 scalable distributed deep-rl with importance weighted actor-learner architectures. In *Proceedings*  
328 *of the 35th International Conference on Machine Learning* (ICML’18, 2018).
- 329 Jesse Farebrother, Joshua Greaves, Rishabh Agarwal, Charline Le Lan, Ross Goroshin, Pablo Samuel  
330 Castro, and Marc G Bellemare. Proto-value networks: Scaling representation learning with  
331 auxiliary tasks. In *The Eleventh International Conference on Learning Representations*, 2023.  
332 URL <https://openreview.net/forum?id=oGDKSt9JrZi>.

- 333 William Fedus, Prajit Ramachandran, Rishabh Agarwal, Yoshua Bengio, Hugo Larochelle, Mark  
334 Rowland, and Will Dabney. Revisiting fundamentals of experience replay. In *International*  
335 *Conference on Machine Learning*, pages 3061–3071. PMLR, 2020.
- 336 Florin Gogianu, Tudor Berariu, Mihaela C Rosca, Claudia Clopath, Lucian Busoni, and Razvan  
337 Pascanu. Spectral normalisation for deep reinforcement learning: An optimisation perspective.  
338 In Marina Meila and Tong Zhang, editors, *Proceedings of the 38th International Conference on*  
339 *Machine Learning*, volume 139 of *Proceedings of Machine Learning Research*, pages 3734–3744.  
340 PMLR, 18–24 Jul 2021.
- 341 Noah Golmant, Nikita Vemuri, Zhewei Yao, Vladimir Feinberg, Amir Gholami, Kai Rothauge,  
342 Michael W Mahoney, and Joseph Gonzalez. On the computational inefficiency of large batch sizes  
343 for stochastic gradient descent. *arXiv preprint arXiv:1811.12941*, 2018.
- 344 Matteo Hessel, Joseph Modayil, Hado van Hasselt, Tom Schaul, Georg Ostrovski, Will Dabney, Dan  
345 Horgan, Bilal Piot, Mohammad Azar, and David Silver. Rainbow: Combining Improvements in  
346 Deep Reinforcement learning. In *Proceedings of the AAAI Conference on Artificial Intelligence*,  
347 2018.
- 348 Łukasz Kaiser, Mohammad Babaeizadeh, Piotr Miłoś, Błażej Osiniński, Roy H Campbell, Konrad  
349 Czechowski, Dumitru Erhan, Chelsea Finn, Piotr Kozakowski, Sergey Levine, Afroz Mohiuddin,  
350 Ryan Sepassi, George Tucker, and Henryk Michalewski. Model based reinforcement learning  
351 for atari. In *International Conference on Learning Representations*, 2020. URL [https://](https://openreview.net/forum?id=S1xCPJHtDB)  
352 [openreview.net/forum?id=S1xCPJHtDB](https://openreview.net/forum?id=S1xCPJHtDB).
- 353 Nitish Shirish Keskar, Dheevatsa Mudigere, Jorge Nocedal, Mikhail Smelyanskiy, and Ping Tak Peter  
354 Tang. On large-batch training for deep learning: Generalization gap and sharp minima. *arXiv*  
355 *preprint arXiv:1609.04836*, 2016.
- 356 Nitish Shirish Keskar, Dheevatsa Mudigere, Jorge Nocedal, Mikhail Smelyanskiy, and Ping Tak Peter  
357 Tang. On large-batch training for deep learning: Generalization gap and sharp minima. In  
358 *International Conference on Learning Representations*, 2017. URL [https://openreview.net/](https://openreview.net/forum?id=H1oyRlygg)  
359 [forum?id=H1oyRlygg](https://openreview.net/forum?id=H1oyRlygg).
- 360 Diederik P. Kingma and Jimmy Ba. Adam: A method for stochastic optimization. In Yoshua  
361 Bengio and Yann LeCun, editors, *3rd International Conference on Learning Representations,*  
362 *ICLR 2015, San Diego, CA, USA, May 7-9, 2015, Conference Track Proceedings*, 2015. URL  
363 <http://arxiv.org/abs/1412.6980>.
- 364 Aviral Kumar, Rishabh Agarwal, Dibya Ghosh, and Sergey Levine. Implicit under-parameterization  
365 inhibits data-efficient deep reinforcement learning. In *International Conference on Learning*  
366 *Representations*, 2021a. URL <https://openreview.net/forum?id=09bnihsFfXU>.
- 367 Aviral Kumar, Rishabh Agarwal, Tengyu Ma, Aaron Courville, George Tucker, and Sergey Levine.  
368 Dr3: Value-based deep reinforcement learning requires explicit regularization. In *International*  
369 *Conference on Learning Representations*, 2021b.
- 370 Sergey Levine, Aviral Kumar, George Tucker, and Justin Fu. Offline reinforcement learning: Tutorial,  
371 review, and perspectives on open problems. *arXiv preprint arXiv:2005.01643*, 2020.
- 372 Long-Ji Lin. Self-improving reactive agents based on reinforcement learning, planning and teaching.  
373 *Mach. Learn.*, 8(3–4):293–321, May 1992.
- 374 Marlos C. Machado, Marc G. Bellemare, Erik Talvitie, Joel Veness, Matthew Hausknecht, and  
375 Michael Bowling. Revisiting the arcade learning environment: Evaluation protocols and open  
376 problems for general agents. *J. Artif. Int. Res.*, 61(1):523–562, jan 2018. ISSN 1076-9757.
- 377 Dominic Masters and Carlo Luschi. Revisiting small batch training for deep neural networks. *ArXiv*,  
378 [abs/1804.07612](https://arxiv.org/abs/1804.07612), 2018.
- 379 Volodymyr Mnih, Koray Kavukcuoglu, David Silver, Andrei A. Rusu, Joel Veness, Marc G. Belle-  
380 mare, Alex Graves, Martin Riedmiller, Andreas K. Fidjeland, Georg Ostrovski, Stig Petersen,  
381 Charles Beattie, Amir Sadik, Ioannis Antonoglou, Helen King, Dharmashan Kumaran, Daan Wierstra,  
382 Shane Legg, and Demis Hassabis. Human-level control through deep reinforcement learning.  
383 *Nature*, 518(7540):529–533, February 2015.

- 384 Evgenii Nikishin, Max Schwarzer, Pierluca D’Oro, Pierre-Luc Bacon, and Aaron Courville. The  
385 primacy bias in deep reinforcement learning. In Kamalika Chaudhuri, Stefanie Jegelka, Le Song,  
386 Csaba Szepesvari, Gang Niu, and Sivan Sabato, editors, *Proceedings of the 39th International  
387 Conference on Machine Learning*, volume 162 of *Proceedings of Machine Learning Research*,  
388 pages 16828–16847. PMLR, 17–23 Jul 2022.
- 389 Max Schwarzer, Ankesh Anand, Rishab Goel, R Devon Hjelm, Aaron Courville, and Philip Bach-  
390 man. Data-efficient reinforcement learning with self-predictive representations. In *International  
391 Conference on Learning Representations*, 2020.
- 392 Christopher J. Shallue, Jaehoon Lee, Joseph Antognini, Jascha Sohl-Dickstein, Roy Frostig, and  
393 George E. Dahl. Measuring the effects of data parallelism on neural network training. *Journal  
394 of Machine Learning Research*, 20(112):1–49, 2019. URL [http://jmlr.org/papers/v20/  
395 18-789.html](http://jmlr.org/papers/v20/shallue18-789.html).
- 396 Ghada Sokar, Rishabh Agarwal, Pablo Samuel Castro, and Utku Evci. The dormant neuron phe-  
397 nomenon in deep reinforcement learning. In *ICML, 2023*.
- 398 Adam Stooke and Pieter Abbeel. Accelerated methods for deep reinforcement learning. *CoRR*,  
399 abs/1803.02811, 2018. URL <http://arxiv.org/abs/1803.02811>.
- 400 Richard S Sutton and Andrew G Barto. *Reinforcement learning: An introduction*. MIT press, 2018.
- 401 Adrien Ali Taiga, William Fedus, Marlos C. Machado, Aaron Courville, and Marc G. Bellemare. On  
402 bonus based exploration methods in the arcade learning environment. In *International Conference  
403 on Learning Representations*, 2020. URL <https://openreview.net/forum?id=BJewlyStDr>.
- 404 Hado P van Hasselt, Matteo Hessel, and John Aslanides. When to use parametric models in re-  
405 inforcement learning? In H. Wallach, H. Larochelle, A. Beygelzimer, F. dAlché-Buc, E. Fox,  
406 and R. Garnett, editors, *Advances in Neural Information Processing Systems*, volume 32. Cur-  
407 ran Associates, Inc., 2019. URL [https://proceedings.neurips.cc/paper/2019/file/  
408 1b742ae215adf18b75449c6e272fd92d-Paper.pdf](https://proceedings.neurips.cc/paper/2019/file/1b742ae215adf18b75449c6e272fd92d-Paper.pdf).
- 409 Christopher JCH Watkins and Peter Dayan. Q-learning. *Machine learning*, 8(3):279–292, 1992.
- 410 Yang Zhao, Hao Zhang, and Xiuyuan Hu. Penalizing gradient norm for efficiently improving  
411 generalization in deep learning. In Kamalika Chaudhuri, Stefanie Jegelka, Le Song, Csaba  
412 Szepesvari, Gang Niu, and Sivan Sabato, editors, *Proceedings of the 39th International Conference  
413 on Machine Learning*, volume 162 of *Proceedings of Machine Learning Research*, pages 26982–  
414 26992. PMLR, 17–23 Jul 2022. URL [https://proceedings.mlr.press/v162/zhao22i.  
415 html](https://proceedings.mlr.press/v162/zhao22i.html).

416 **Broader impact** Although the work presented here is mostly of an academic nature, it aids in the  
417 development of more capable autonomous agents. While our contributions do not directly contribute  
418 to any negative societal impacts, we urge the community to consider these when building on our  
419 research

## 420 A Related work

421 There is a considerable amount of literature on understanding the effect of batch size in supervised  
422 learning settings. [Keskar et al. \[2016\]](#) presented quantitative experiments that support the view that  
423 large-batch methods tend to converge to sharp minimizers of the training and testing functions, and as  
424 has been shown in the optimization community, sharp minima tends to lead to poorer generalization.  
425 [Masters and Luschi \[2018\]](#) support the previous finding, presenting an empirical study of stochastic  
426 gradient descent’s performance, and reviewing the underlying theoretical assumptions surrounding  
427 smaller batches. They conclude that using smaller batch sizes achieves the best training stability  
428 and generalization performance. Additionally, [Golmant et al. \[2018\]](#) reported that across a wide  
429 range of network architectures and problem domains, increasing the batch size yields no decrease in  
430 wall-clock time to convergence for either train or test loss.

431 Although batch size is central to deep reinforcement learning algorithms, it has not been extensively  
432 studied. One of the few results in this space is the work by [Stooke and Abbeel \[2018\]](#), where they  
433 argued that larger batch sizes can lead to improved performance when training in distributed settings.  
434 Our work finds the opposite effect: *smaller* batch sizes tends to improve performance; this suggests  
435 that empirical findings may not directly carry over between single-agent and distributed training  
436 scenarios.

437 [Fedus et al. \[2020\]](#) presented a systematic and extensive analysis of experience replay in Q-learning  
438 methods, focusing on two fundamental properties: the replay capacity and the ratio of learning  
439 updates to experience collected (e.g. the replay ratio). Although their findings are complementary to  
440 ours, further investigation into the interplay of batch size and replay ratio is an interesting avenue  
441 for future work. Finally, there have been a number of recent works investigating network plasticity  
442 [[Nikishin et al., 2022](#), [D’Oro et al., 2023](#), [Sokar et al., 2023](#)], but all have kept the batch size fixed.

## 443 B Code availability

444 Our experiments were built on open source code, mostly from the Dopamine repository. The root  
445 directory for these is <https://github.com/google/dopamine/tree/master/dopamine/>, and we specify the  
446 subdirectories below (with clickable links):

- 447 • DQN, Rainbow, QR-DQN and IQN agents from [/jax/agents/](#)
- 448 • Atari-100k agents from [/labs/atari-100k/](#)
- 449 • Batch size from [/jax/agents/quantile/configs/quantile.gin](#) (**line 36**)
- 450 • Exploration  $\epsilon = 0$  from [/jax/agents/quantile/configs/quantile.gin](#) (**line 16**)
- 451 • Resnet from [/labs/offline-rl/jax/networks.py](#) (**line 108**)
- 452 • Dormant neurons metric from [/labs/redo/](#)

453 For the srnk metric experiments we used code from:  
454 [https://github.com/google-research/google-research/blob/master/](https://github.com/google-research/google-research/blob/master/generalization_representations_rl_aistats22/coherence/coherence_compute.py)  
455 [generalization\\_representations\\_rl\\_aistats22/coherence/coherence\\_compute.py](https://github.com/google-research/google-research/blob/master/generalization_representations_rl_aistats22/coherence/coherence_compute.py)

## 456 C Atari 2600 games used

457 Most of our experiments were run with 20 games from the ALE suite [[Bellemare et al., 2013](#)], as  
458 suggested by [Fedus et al. \[2020\]](#). However, for the Atari 100k agents ([subsection 3.3](#)), we used the  
459 standard set of 26 games [[Kaiser et al., 2020](#)] to be consistent with the benchmark. Finally, we also  
460 ran some experiments with the full set of 60 games. The specific games are detailed below.



461 **20 game subset:** AirRaid, Asterix, Asteroids, Bowling, Breakout, DemonAttack, Freeway, Gravitar,  
462 Jamesbond, MontezumaRevenge, MsPacman, Pong, PrivateEye, Qbert, Seaquest, SpaceInvaders,  
463 Venture, WizardOfWor, YarsRevenge, Zaxxon.

464 **26 game subset:** Alien, Amidar, Assault, Asterix, BankHeist, BattleZone, Boxing, Breakout, Chop-  
465 perCommand, CrazyClimber, DemonAttack, Freeway, Frostbite, Gopher, Hero, Jamesbond, Kanga-  
466 roo, Krull, KungFuMaster, MsPacman, Pong, PrivateEye, Qbert, RoadRunner, Seaquest, UpNDown.

467 **60 game set:** The 26 games above in addition to: AirRaid, Asteroids, Atlantis, BeamRider, Berzerk,  
468 Bowling, Carnival, Centipede, DoubleDunk, ElevatorAction, Enduro, FishingDerby, Gravitar, Ice-  
469 Hockey, JourneyEscape, MontezumaRevenge, NameThisGame, Phoenix, Pitfall, Pooyan, Riverraid,  
470 Robotank, Skiing, Solaris, SpaceInvaders, StarGunner, Tennis, TimePilot, Tutankham, Venture,  
471 VideoPinball, WizardOfWor, YarsRevenge, Zaxxon.

472 **D Second order optimizer effects.**

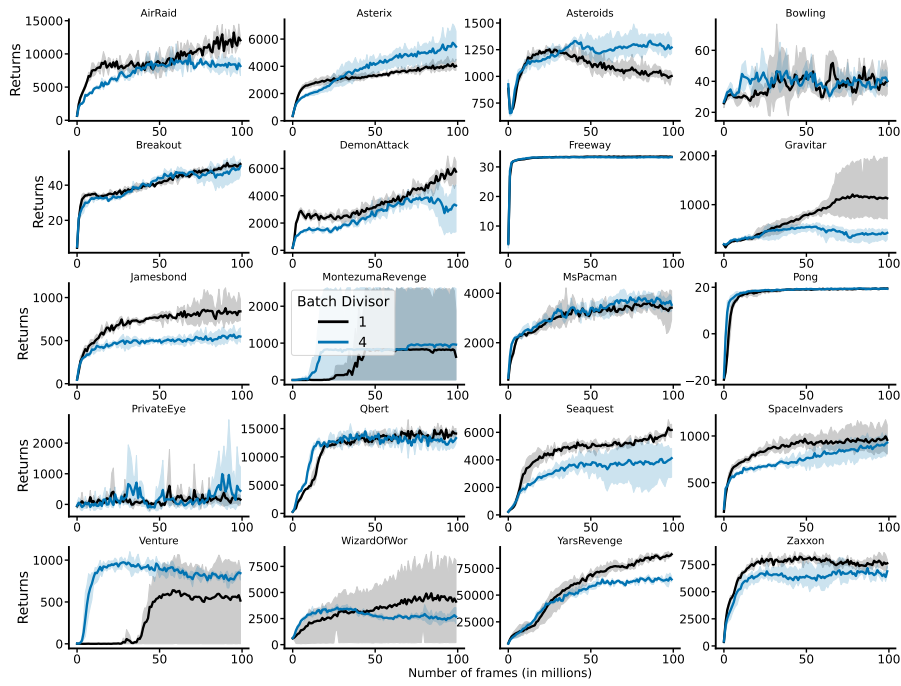


Figure 13: Evaluating multiple gradient updates per training step on QR-DQN, training curves for all games.

473 **E Variance of updates.**

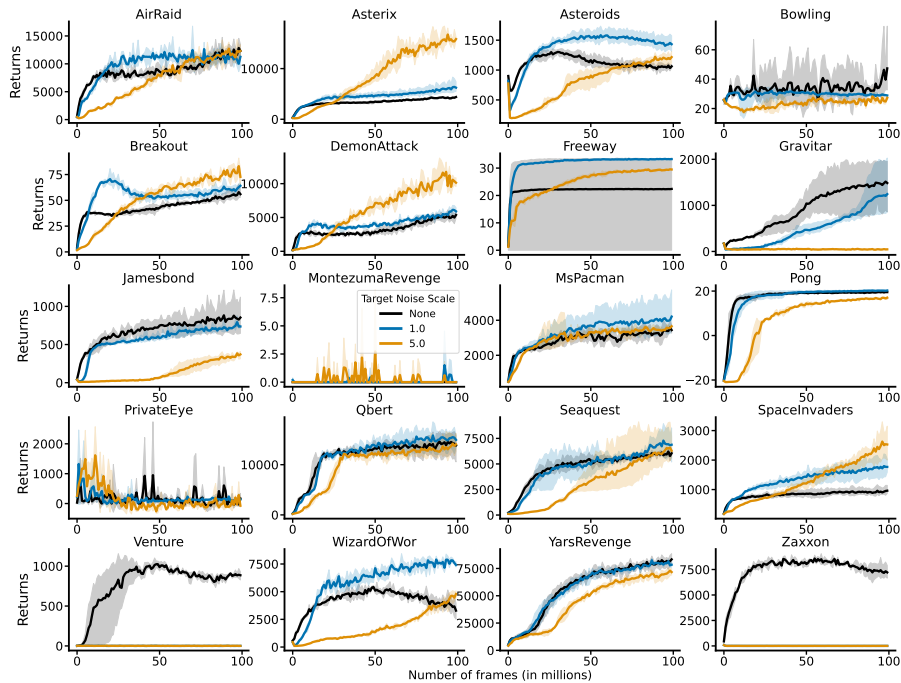


Figure 14: Evaluating the effect of adding target noise to QR-DQN, learning curves for all games.

474 **F Results on the full ALE suite**

475 We additionally provide complete results for all games using QR-DQN agent in Figure 15.

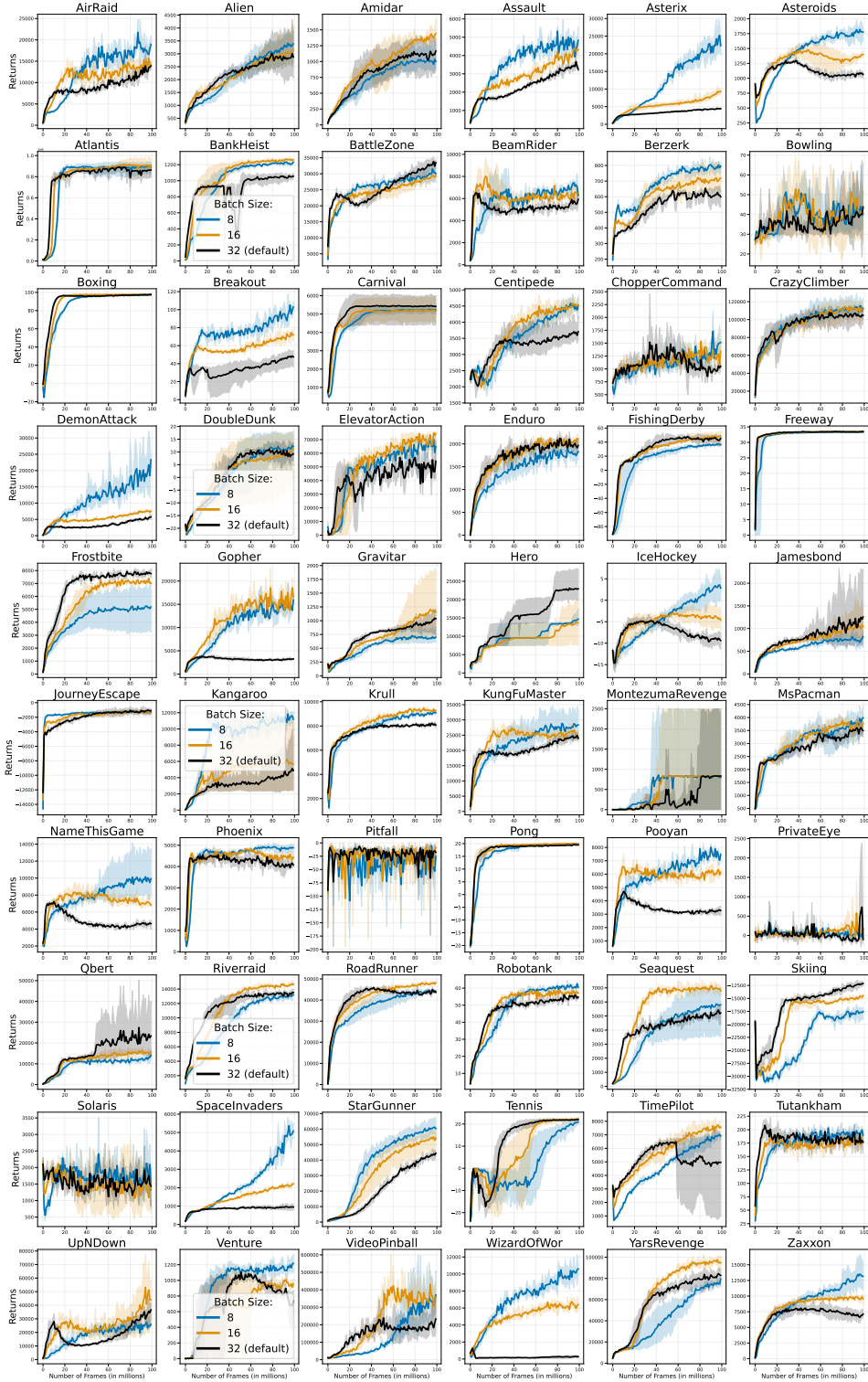


Figure 15: Training curves for QR-DQN agent. The results for all games are over 3 independent runs.

476 **G Varying architectures**

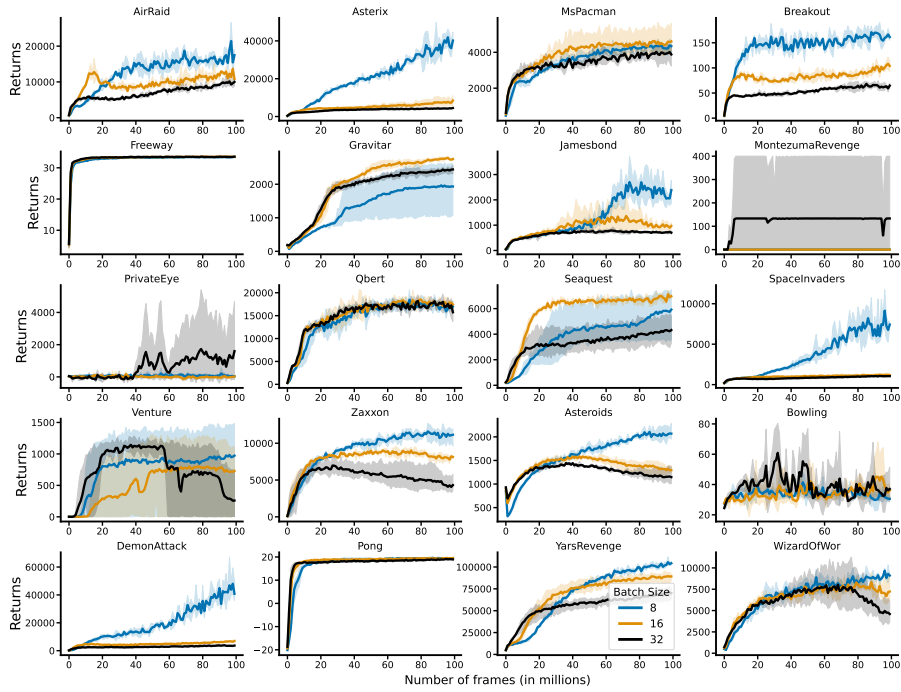


Figure 16: Evaluating the effect of CNNx4 to QR-DQN, learning curves for all games.

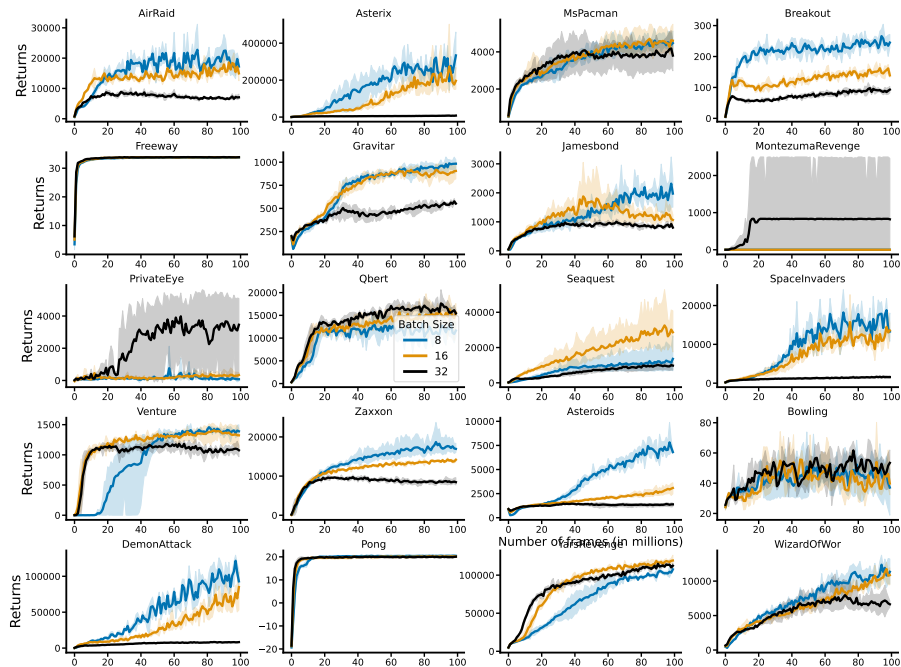


Figure 17: Evaluating the effect of Resnet to QR-DQN, learning curves for all games.

477 **H Training Stability**

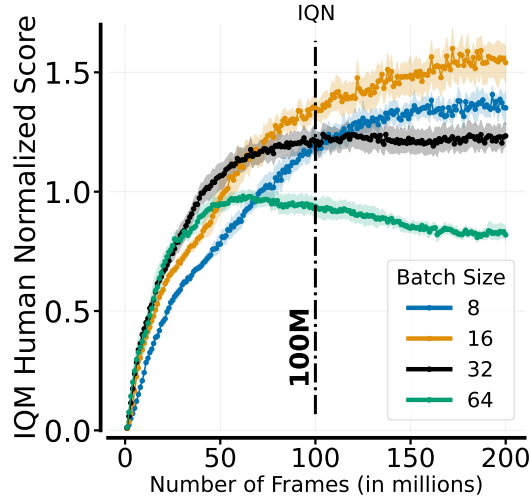


Figure 18: Measuring IQM for human-normalized scores when training for 200 million frames using IQN [Dabney et al., 2018b]. Results aggregated over 20 games, where each experiment was run with 3 independent seeds and we report 95% confidence intervals.

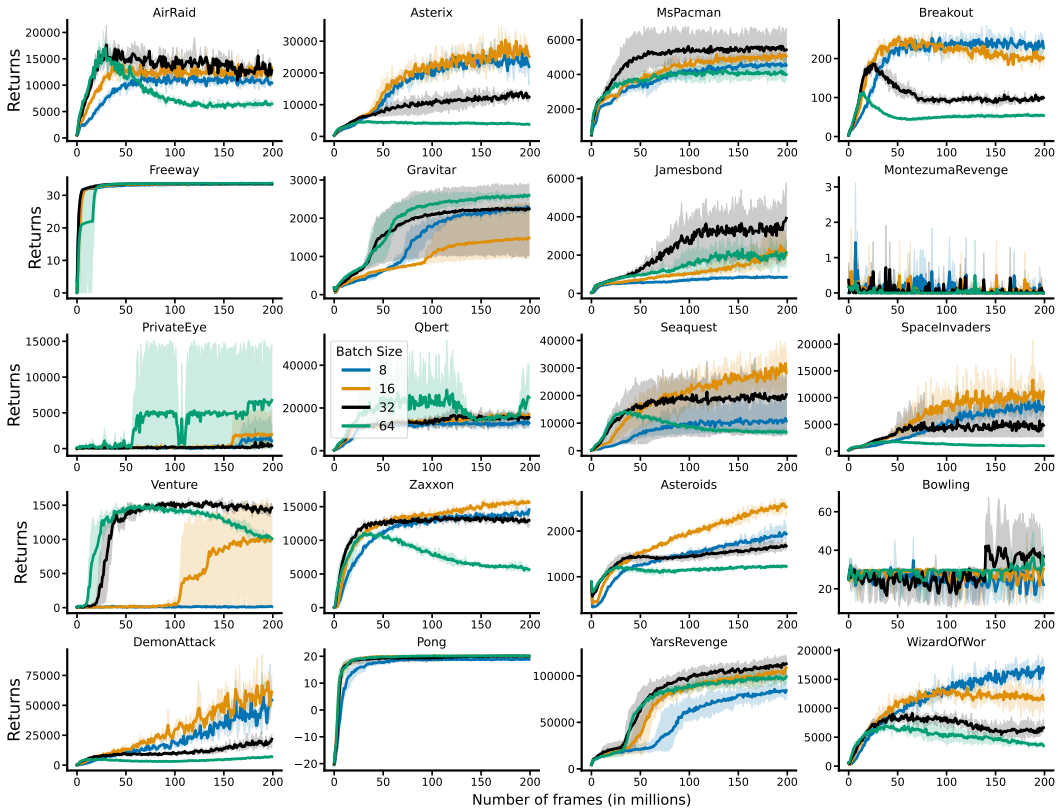


Figure 19: Learning curves for individual games, when trained for 200 million frames using IQN [Dabney et al., 2018b]. Results aggregated over 3 seeds, reporting 95% confidence intervals.



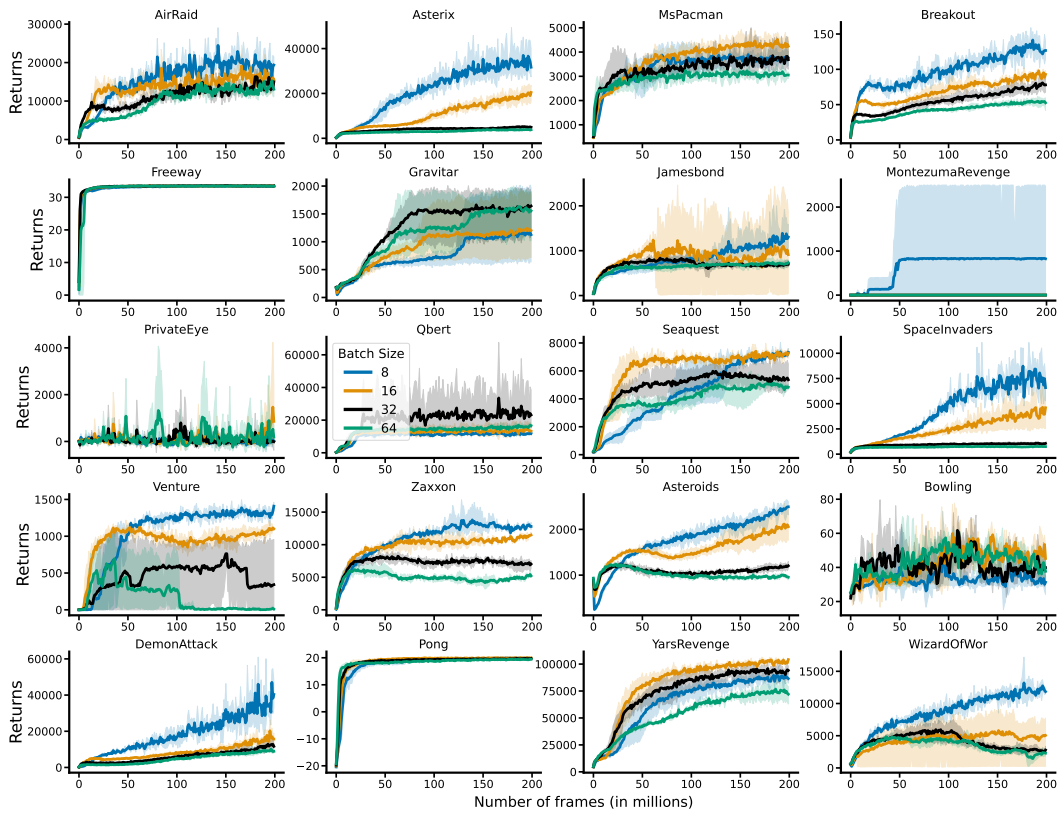


Figure 20: Learning curves for individual games, when trained for 200 million frames using QR-DQN [Dabney et al., 2018a]. Results aggregated over 3 seeds, reporting 95% confidence intervals.